Appl. Phys. B 87, 139–144 (2007)
DOI: 10.1007/s00340-006-2563-9

Applied Physics B
Lasers and Optics

H. EL-RABII[1,✉]
G. GABOREL[2]

Laser ignition of flammable mixtures via a solid core optical fiber

[1] Laboratoire de Combustion et de Détonique, 1 av. Clément Ader, B.P. 40109, 86961 Chasseneuil-Futuroscope, France
[2] Vibro-Meter France, 8 Chemin de l'étang, B.P. 15, 16730 Fléac, France

Received: 9 September 2006/
Revised version: 24 November 2006
Published online: 31 January 2007 •

ABSTRACT To date no commercial fiber coupled laser systems have reached the irradiance and pulse energy required for flammable mixtures ignition. In this work we report preliminary results on the ignition of two-phase mixtures promoted by a laser delivering pulses through optical fiber. Experiments undertaken on free beam path configurations have allowed identification of the optical parameters required for laser ignition. The fiber coupled system used is based on a Q-switched nanosecond laser operating at 1064 nm. The fiber input angle and the focal length have been identified as the most important parameters. We demonstrated the possibility of delivering nanosecond pulses of 30 mJ focused onto a spot of 200 μm through a solid core optical fiber, and to promote ignition of *n*-heptane/air and JP4/air mixtures.

PACS 42.62.-b; 42.81.-i; 47.55.-t; 82.33.Vx

1 Introduction

Ignition of flammable mixtures is of fundamental interest and of crucial practical importance in a wide range of combustion applications. In most situations it is accomplished with an electrical discharge. Such a discharge is a fairly effective means to convert electrical energy to heat since only a weak portion of the deposited energy is dissipated in the form of radiation and sound waves. However, in certain applications, traditional spark plugs may not be the most suited solution to promote ignition.

A typical problem which has motivated the search for alternative ignition sources is the critical temperature and pressure conditions encountered at high-altitudes under which jet engines operate. Such conditions considerably reduce the stability of the gas turbine combustor, leading in the worst case, to flame extinction. When this occurs, the ignition device should be able to ensure relighting despite the higher minimum ignition energy needed and the modification of the flow pattern at high altitude.

Furthermore, the search for better efficiency performance has led the aeronautical industry to develop engines with higher compression ratio and higher primary-zone velocities. These changes call for larger spark plug voltage to ignite the highly turbulent mixtures flowing through the combustor. But the more energy released by sparks the higher the rate of erosion of the electrodes and the semiconductor which can lead to an increase of the gap between electrodes requiring then higher voltage for sparking. In the most serious cases, the contact between the electrodes and the semiconductors can be broken making the ignition unit unusable. Besides, experience has shown that adverse environmental conditions of the ignition unit also play a role in the deterioration of the electrodes, shortening their lives. Finally, the design of an ignition system operating during the full engine life would allow for minimum maintenance costs.

Several options have been proposed to overcome these severe drawbacks. Laser ignition seems to be one of the most promising alternatives and has been already the subject of numerous studies [1–10]. The major benefits of this solution are the long-lasting performance of laser systems, the absence of quenching effects due to the spark plug electrode, the precise ignition timing, and the easy regulation of the deposited energy. The use of specific optical converging system may allow one to obtain an optimal flame-front area-to-volume ratio, thereby lowering the optimal combustion mixture to the fuel lean side, and hence decreasing the emission of pollutants. Probably the most attractive benefit is the possibility of initiating combustion in desired spatial regions. The main difficulty, beside cost and mechanical issues, concerns the delivery system to use. A free beam path configuration is not an acceptable solution as it carries safety and reliability issues. Optical fibers inevitably appears as an obvious means to ensure transmission of laser energy. Still their uses are not straightforward, and despite the critical importance of this issue only limited work was devoted to the transmission of nanosecond optical pulses suitable for ignition through optical fibers. Stakhiv et al. [11] tested several kind of fibers to identify candidates for practical use. The group failed to obtained non destructive propagation of nanosecond pulses without deteriorating the beam quality of the delivered pulses to a nonpermissible amount for gas breakdown. Although hollow-core photonic crystal fiber was identified as a good candidate for this application no gas-phase sparks were reported in their paper. Other studies reported successful transmission of picosecond pulse trains through hollow-core photonic-crystal fibers but

✉ Fax: +33 5 49498291, E-mail: hazem.elrabii@lcd.ensma.fr

also without reporting spark formation in the gas phase [12]. The first delivery of nanosecond laser pulses through a flexible fiber (cyclic olefin polymer coated silver hollow fiber) to produce optical sparks in atmospheric-pressure gases was reported by Yalin et al. [13].

In this paper, we study the laser ignition of two-phase mixtures involving *n*-heptane and JP4. Tests were performed in two different configurations which will be described later on. Our objective is to identify under which conditions laser ignition of *n*-heptane/air and JP4/air mixtures is obtained and to demonstrate the possibility of using a solid core fiber coupled laser system to deliver a laser pulse to a combustion chamber. The delivering optical system is described, which includes the kind of fiber used, the appropriate launch conditions, and the optical focusing system used.

2 Experimental results

2.1 *Free beam path configuration*

The experimental set-up is presented in Fig. 1. The laser-induced spark was produced by a Quantel Ultra Nd-YAG laser operating as a Q-switched laser. It delivered pulses of 6 ns (FWMH) duration at 1064 nm with a repetition rate of up to 20 Hz. The beam presented a diameter (86.5% of the energy) and a divergence (86.5% of the energy) respectively of 2.8 mm and 0.6 mrad. The laser energy was controlled by using a pair of glan calcite polarizers. While maintaining a fixed polarization state, the incident energy was systematically varied by adjusting the relative angle between the two polarizers.

Breakdown was achieved by using a BK7 bi-concave lens (−75 mm) followed by a BK7 bi-convex lens (75.6 mm). The distance between the two lenses was chosen to optimize the breakdown (a condition obtained for 240 mm). The incident and transmitted pulse energies were measured using two pyroelectric energy meters. Incident pulse energies were measured by splitting-off a fraction of the laser pulse energies. The transmitted pulses energies were collected and collimated by a BK7 converging lens before reaching the second head. During the experiments, the laser sparks were created 10 mm above the nose of the spray generator.

Atomization of the liquid fuel was achieved by a 40 kHz ultrasonic atomizer. The fuel was dispensed to the probe through a mass-flow meter/controller (maximum scale: 0.5 l/h) calibrated for *n*-heptane. The vessel containing the fuel was pressurized with helium and the burner was fed with air through a mass flow meter/controller (maximum scale: 4 m_n^3/h). The atomization chamber consists of a pyrex tube, making it possible to visualize the spray. The chamber is closed at the top by a 10 mm diameter aperture and at the bottom by a plate allowing the gas and liquid connection and the plug-in of the spray device. The non-vibrating part of the sprayer is fixed on a plate whose orientation is adjustable using three independent screws.

Particle sizes in the spray were measured by phase-doppler anemometry (PDA) in a previous study [14]. All measurements were carried out with water. The volume of measurement was moved in a vertical plane containing the atomizer axis. For each position, the distribution of droplet sizes was obtained. Measurements were based on samples of typically 10^4 drops. The distribution of the droplet diameters was particularly narrow with 90% having their diameters ranging between 25 and 45 μm (Fig. 2).

The droplet diameters, D, for the fuels used in the present study with the same atomizer were deduced according to the following relation [15]

$$\frac{D_{\text{fuel}}}{D_{\text{H}_2\text{O}}} = \frac{(\sigma/\varrho)^{1/3}_{\text{fuel}}}{(\sigma/\varrho)^{1/3}_{\text{H}_2\text{O}}}, \tag{1}$$

where σ and ϱ stand respectively for the surface tension and the density of the liquid considered. We obtain for the droplet cloud of *n*-heptane and JP4 a mean diameter of 31 μm.

Figure 3 presents transmitted energy versus incident energy for different *n*-heptane/air mixtures. The composition of the different mixtures are presented in Table 1. Each measurement point corresponds to a single shot event. The outlet velocity was 4.2 m/s in all cases, except for mixture 1 for which the speed of the air flow was 8.5 m/s. These values correspond respectively to a Reynolds number of 2930 and 5930.

These results illustrate that, for all equivalence ratios under consideration, a sufficient level of laser energy was

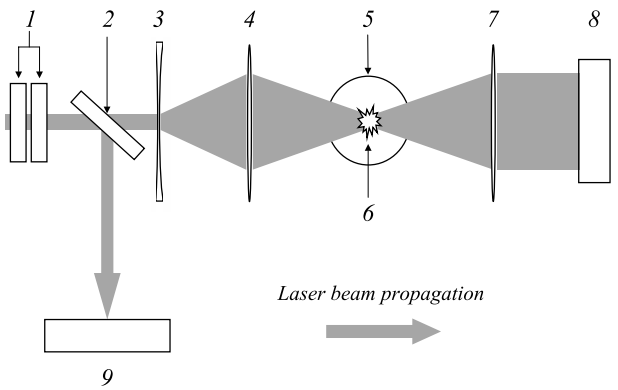

FIGURE 1 Experimental setup: 1 pair of glan calcite polarizers, 2 beam-splitter, 3 bi-concave lens, 4 bi-convex lens, 5 atomization chamber, 6 laser spark, 7 bi-convex collecting lens, 8 and 9 energymeters

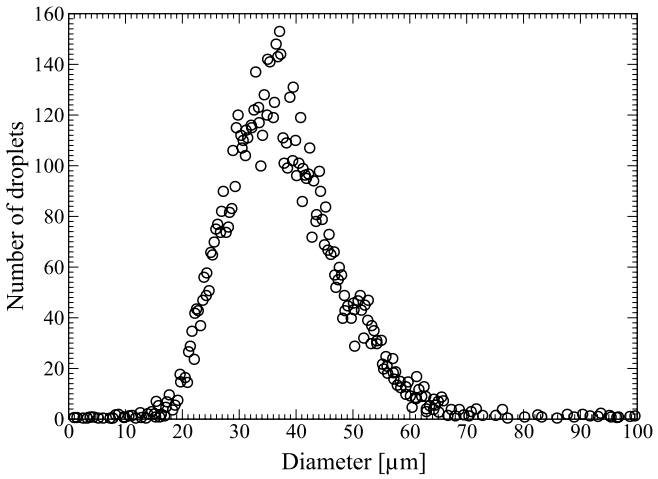

FIGURE 2 Droplet size distribution 8 mm from the atomization surface

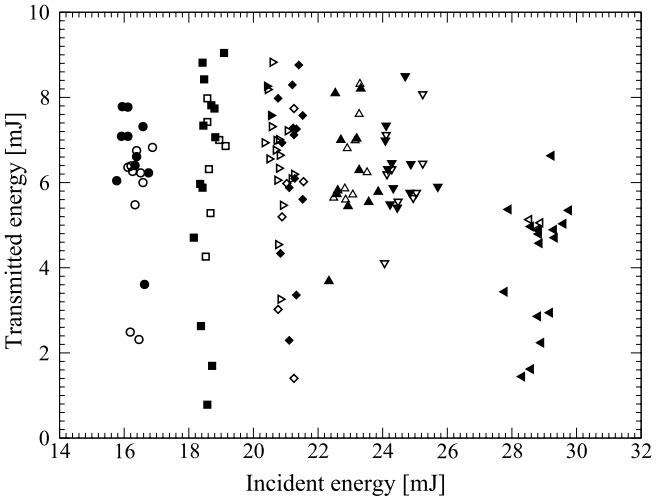

FIGURE 3 Transmitted versus incident energy for *n*-heptane/air mixtures. Empty and filled symbols correspond respectively to successful and unsuccessful ignition events. Mixture 1 (▷, ▶), mixture 2 (○, ●), mixture 3 (□, ■), mixture 4 (◇, ◆), mixture 5 (△, ▲), mixture 6 (▽, ▼), and mixture 7 (◁, ◀)

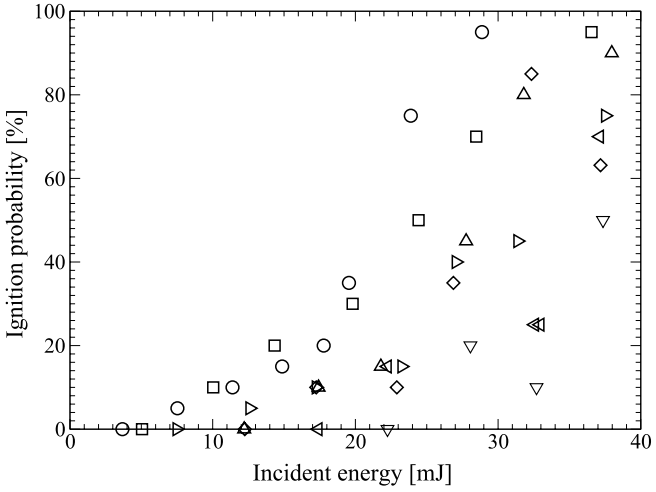

FIGURE 4 Ignition probability versus incident energy for JP4/air mixtures. Mixture 1 (○), mixture 2 (□), mixture 3 (◇), mixture 4 (△), mixture 5 (▽), mixture 6 (◁), and mixture 7 (▷)

Mixture	*n*-heptane		JP4	
	Air flowrate (kg/h)	Fuel flowrate (kg/h)	Air flowrate (kg/h)	Fuel flowrate (kg/h)
1	3.1	6.8×10^{-2}	1.03	4.5×10^{-2}
2	1.6	6.8×10^{-2}	1.03	9.0×10^{-2}
3	1.6	1.03×10^{-1}	1.03	1.4×10^{-1}
4	1.6	1.03×10^{-1}	1.03	1.8×10^{-1}
5	1.6	1.03×10^{-1}	3.10	9.0×10^{-2}
6	1.6	1.37×10^{-1}	3.10	1.4×10^{-1}
7	1.6	1.71×10^{-1}	3.10	1.8×10^{-1}

TABLE 1 Composition of the different fuel/air mixtures

available to ignite the mixtures. A laser pulse energy ranging from 16 to 29 mJ was necessary to promote ignition. The absorption, which corresponds to the ratio of the incident energy minus the transmitted energy with the incident energy, presents strong fluctuations. An absorption of at least 50% has been achieved in all our tests. Values up to 97% were obtained in the case of the mixture presenting an equivalence ratio of 1.0 (squares in Fig. 3).

Ignition probability versus incident energy for JP4/air mixtures is presented in Fig. 4. Ignition probabilities were obtained from a sample of 20 shots. As in the case of *n*-heptane/air mixtures, the incident energy necessary to obtain ignition increases with the fuel percentage. For mixtures 1, 2 and 3, 50% of the shots promoted ignition for incident energies respectively of 22, 24 and 28 mJ. For mixture 4, an incident energy of about 28 to 32 mJ was also sufficient to ignite it. In the case of leaner mixtures (5, 6 and 7), more energy was necessary, typically about 35 mJ, in order to balance the losses due to the higher speed of the flow at the outlet of the burner.

2.2 *Fiber laser coupled configuration*

The above-described experiments have shown that minimum pulse energies leading to breakdown and ignition are higher than 16 mJ, corresponding to irradiances higher than 0.4 GW/cm^2. Transmitting such high peak power pulses through optical fibers proved to be very difficult. Single mode optical fibers are limited in power density by their small diameter core, reducing the maximum peak power acceptable to a few kilowatts. Recently large mode area fibers have been developed for fiber laser by reducing the index difference between the core and the cladding, allowing only for lower order modes to propagate [16]. Fibers with 21 μm core have been able to deliver pulses of 150 mJ (corresponding peak powers are > 100 kW). The limitations of this approach are the fiber bend losses due to the lower numerical aperture and the silica damage threshold which is < 5 GW/cm^2.

Newly developed hollow-core photonic band gaps fibers (see [17]) were also investigated. It basically consists of a core filled with air and surrounded by a two-dimensionally periodic structure of air/holes which acts as a highly reflective Bragg reflector for discrete regions (or band gaps) of the electromagnetic spectrum. The generation of solitons with peak powers greater than 5.5 mW (pulse energy of 450 nJ) in such Xe-filled fiber was obtained [19]. However, this peak power has not been so far reproduced for the picosecond and nanosecond regime, limiting the energy level to well below what is required for laser spark ignition.

A solution using a cyclic olefin polymer-coated hollow (COPCH) fiber was used by Yalin et al. [13] for laser ignition. It makes use of the propagation of a low numerical aperture laser beam through a multimode fiber. Unlike silica/silica fiber, the COPCH fiber used was made of a hollow quartz tube (700 μm diameter) with an inner diameter coated with silver and polymer acting as a dielectric reflector. A straight hollow core enables transmission of pulses with higher energy without a serious deterioration of its spatial properties [13].

We tested multimode optical fibers of different core sizes to determine their maximum pulse energy transmission. The setup used during the tests for focusing the Q-switched Nd:YAG laser into a 150 cm-long fiber is presented in Fig. 5. Special attention was taken when coupling the laser beam into the optical fiber in order to allow only propagation of the lowest order modes. The 2.8 mm diameter beam was focused 20 mm before the fiber, using a 100 mm focal length lens in order to cover most of the core area and thus to prevent

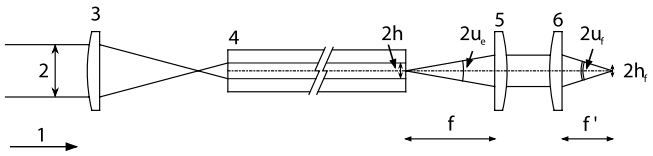

FIGURE 5 Fiber coupling and optical plug: 1 laser beam propagation direction, 2 initial beam diameter (2.8 mm), 3 coupling lens ($f = 100$ mm), 4 optical fiber, 5 collecting lens, 6 focusing lens

input face damage (Fig. 5). The launch numerical aperture was 0.014 rad, which was much less than the fiber numerical aperture (0.22 rad). The focal spot diameter 20 mm in front of the fiber was 47 μm which, for 50 mJ pulses, corresponds to an irradiance of 5×10^{11} W/cm^2. This value is very close to the threshold intensity of air and to prevent spark formation in the fiber, the fiber coupling was sealed in an enclosure purged with helium. The maximum average core intensities measured and presented in Table 2 are consistent with the maximum intensities given by fiber manufacturers. We see that a fiber with a core size of 940 μm is able to transmit pulses up to 45 mJ. It is important to note that fiber core intensities reported in Table 2 are sufficient for liquid ignition but insufficient for igniting a gas mixture at atmospheric pressure because the threshold ignition irradiance for a gas mixture is one or two orders of magnitude higher than that for igniting a liquid mixture. Although these core intensities are all lower than the optical threshold damage for all existing solid-core fibers, fiber damage by randomly occurring hot spots in laser profiles are nevertheless possible. This seems to indicate that solid-core fiber is not the best candidate for laser ignition applications as pointed out in [18]. However, solid-core fibers are easily available and present the ability to withstand high-temperatures when coated with metallic coatings, which greatly justify the choice of this kind of fiber in the present study.

The nature of light leaving the fiber is partially coherent and corresponds to the contribution of all coherent modes leaving the fiber. The more higher orders that leave the fiber the more difficult it is to focus the exiting beam. The power coupled into those modes have a higher divergences and could fall outside the clear aperture of collimating lens. The focused spot diameter is given by the optical design but the amount of light falling into that spot is given by the launch conditions and the fiber curvature. The fiber's bends are responsible for the shifting of the power transmitted to higher order modes. This is why the launch conditions and the fiber curvature are critical for breakdown and ignition. To be closer to real situations, from then on, the fiber was bent at an angle of 90° with a radius of curvature of 50 cm. Measurement of the exiting beam numerical aperture gave 0.033 rad.

Core diameter (μm)	Maximum pulse energy (mJ)	Average core intensity (GW/cm^2)
200	3	1.4
400	15	1.7
940	45	0.9

TABLE 2 Maximum transmitted energy against the fiber core diameter

To determine the focused spot size and optimize the system, we calculated the image formation of the fiber's end face at the image plane using geometrical optics while taking into account aberration introduced by high numerical aperture lenses. According to Lagrange's invariant, the products of the image/object height, (h_f, h), by the angles of incidence, $(u_\mathrm{f}, u_\mathrm{e})$, and the refractive indexes in the image and the object, (n', n), are constant. Since these refractive indexes are the same, the focal spot radius is given by:

$$h_\mathrm{f} = h\frac{\sin u_\mathrm{e}}{\sin u_\mathrm{f}} \,. \tag{2}$$

Assuming paraxial approximation and a parallel beam of light between the collecting and the focusing lens we have:

$$h_\mathrm{f} = h\frac{f'}{f} \,, \tag{3}$$

where f, f' correspond respectively to the focal length of the collecting and the focussing lens.

The spot size is then proportional to the core size of the optical fiber and to the ratio between the focusing and the collecting lenses. The core diameter was chosen according to the maximum power transmission and could not be reduced further. The remaining possibility for reducing the diameter of the spot size was therefore to reduce the ratio f'/f. The diameter of the optical plug being limited by the access to the combustion chamber to 1 cm, a 75 mm-focal length lens was used to collect the light and was set 75 mm downstream of the fiber. Increasing the focal distance of the collecting lens was therefore only possible if the beam divergence at the output of the fiber could be further reduced.

Three different optical plugs were constructed using three different focusing lenses, influencing the spark location and the intensity. Two plano-convex lenses ($f' = 10$ and 20 mm) made of sapphire were picked for their ability to withstand the high temperature and pressure of the combustion chamber. The third lens was aspheric ($f' = 8$ mm) in order to form the smallest possible image by compensating the spherical aberrations introduced by the high numerical aperture lens (0.5). We characterized the beam at different locations along the beampath with an optical beam profiler. For illustrative purpose, we present in Fig. 6 the beam profile at four different locations: upstream of the coupling lens (Fig. 6a), at the input face of the fiber (Fig. 6b), at the exit of the fiber (Fig. 6c), and at the focal point of the system when using the 20 mm-focal lens (Fig. 6d). The spatial profile of the beam exiting the fiber was clearly multimode as shown in Fig. 6c. We measured the M^2 of the beam entering the fiber, the launch input half-angle (u_i), the beam waist and the intensity at the fiber input face (h_i, I_i), the exit half-angle of the beam leaving the fiber (u_e), as well as the beam waists and the intensities at the focal point for each focusing optics (h_f, I_f). All reported intensities in the present work assume a circular beam area with radius equal to the beam waist. The experimental results are summarized in Table 3. We found that the laser used presented a near-diffraction-limited spatial quality with an $M^2 \simeq 1.6$. The beam radius at the entry fiber face was 250 μm, which corresponds to an averaged intensity of 3.8×10^9 W/cm^2, and agrees well with the calculated value. At the focal point of the whole system, radii

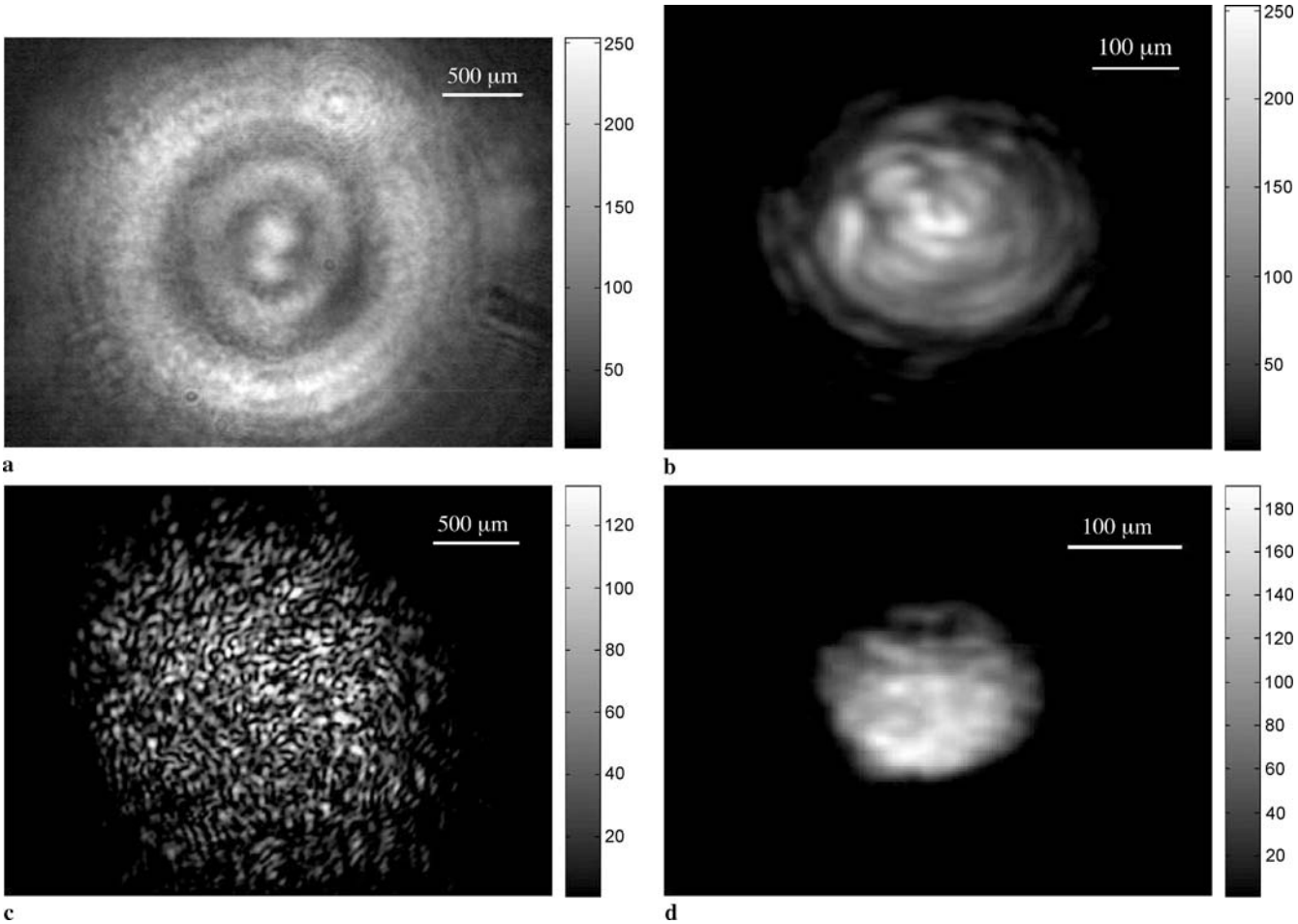

FIGURE 6 Beam profile at different locations along the beampath. (**a**) Upstream of the coupling lens. (**b**) Entrance face of the fiber. (**c**) Exit of the fiber. (**d**) Focal point of the 20 mm-focal lens

			Calculated values				Measured values					
h (µm)	f (mm)	f' (mm)	u_f (mrad)	h_f (µm)	I_f (GW/cm^2)	M^2	u_i (mrad)	u_e (mrad)	u_f (mrad)	h_f (µm)	I_i (GW/cm^2)	I_f (GW/cm^2)
470	75	8	0.319	50	64	1.6	14	34	38	50	38	63.7
470	75	10	0.249	62.5	41	1.6	14	34	30	67	38	35.5
470	75	20	0.126	125	10	1.6	14	34	15	110	38	13.2

TABLE 3 Calculated and measured beam parameters

of 50, 67, and 110 µm were found for the 8 mm-, 10 mm-, and 20 mm-focal lens, respectively. Breakdown and ignition measurements were conducted with transmitted pulse energies of 30 mJ (input energies of 52 mJ), which corresponds to averaged intensities of 6.37, 3.55, and 1.32×10^{10} W/cm^2, respectively (see Fig. 7). Once again, these values are in good agreement with the calculated one. Figure 7 also shows that the increase of the curvature decreases the optical intensity reaching the desired spark location.

We first verified if air breakdown could be achieved with any of the three focal lengths. The breakdown was produced in a closed vessel filled with air at three different pressures: 1, 4, and 6 bar. Results are presented in Table 4. As expected, at atmospheric pressure, for most laser shots no sparks were observed. Only sporadic sparks were obtained for the 8 mm and the 10 mm focal lengths, probably due to the presence of dust at the focal point. At elevated pressures the breakdown probability increases appreciably, reaching 50% at 4 bar and 90% at 6 bar with the 8 mm-focal length lens. These results confirm the impossibility of producing non-resonant breakdown in air at atmospheric pressure with a solid core optical fiber. Only for high pressures and for a small focal length ratio f'/f was air breakdown achieved.

After having conducted the described experiments, we finally tested the ability of the fiber-coupled configuration to promote ignition of two-phase mixtures. The tests were carried out with droplets of *n*-heptane mixed with air using the atomization chamber described in Sect. 2.1. The energy pulse was set to 30 mJ at the exit of the fiber coupled laser ignition system and was not varied during all the tests. Ignition was carried out with the 20 mm focal length. The tip of the optical spark plug was placed 20 mm away from the cloud of droplets whilst the focal point was located at the interface with the droplets cloud. Preliminary results show that about

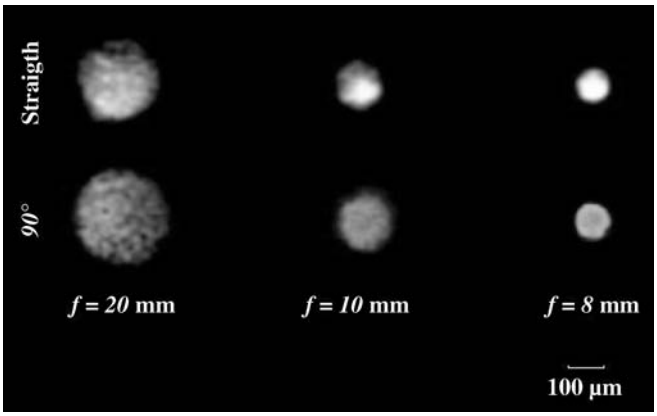

FIGURE 7 Beam profiles at the focal point for $f = 20$, 10, and 8 mm-focal length lens, for straight and curved fiber

f' (mm)	$p_{air} = 1$ bar	$p_{air} = 4$ bar	$p_{air} = 6$ bar
8	< 1%	50%	90%
10	< 1%	10%	50%
20	0%	0%	< 1%

TABLE 4 Air breakdown probability against pressure

80% of shots were successful in igniting the mixture at a distance of 20 mm from the cloud of droplets while electrical sparks were not sufficiently close to reliably ignite the mixture (20% ignition success). This clearly demonstrate the main advantage of laser ignition over the traditional means largely due to the ability to freely locate the optical spark within the spray.

3 Conclusion

In the present study, we have demonstrated the possibility of igniting a two-phase reactive mixture involving a liquid fuel with a laser spark. Two configurations have been considered: a beam free path and fiber transmitted pulses configuration.

The beam free path experiments have shown that the minimum incident energy level leading to ignition lies between 16 and 30 mJ. Although no sparking was recorded in air at atmospheric pressure, for the fiber transmitted pulses configuration, the irradiance was sufficient to promote sparking on fuel droplets, and to ignite different fuel/air mixtures involving *n*-heptane. However, at pressures above 4 bar it was possible to produce sparks in air. It was shown that the launch conditions and the fiber curvature were critical for spark ignition. The focused spot diameter was given by the optical design while the amount of light falling into that spot was given by the launch conditions and fiber curvature. These first results are quite encouraging and may represent a significant progress toward the design of a robust laser ignition unit.

REFERENCES

1 J. Syage, E. Fournier, R. Rianda, R. Cohen, J. Appl. Phys. **64**, 1499 (1988)
2 T. Spliganin, A. McIlroy, E. Fournier, R. Cohen, J. Syage, Combust. Flame **102**, 310 (1995)
3 Y.-L. Chen, J. Lewis, C. Parigger, J. Quant. Spectrosc. Radiat. Transf. **66**, 41 (2000)
4 Y.L. Chen, J. Lewis, C. Parigger, Opt. Express **9**, 360 (2001)
5 H. El-Rabii, J.C. Rolon, *Advances in Combustion and Atmospheric Pollution* (Torus-Press, Moscow, 2004)
6 T. Phuoc, F. White, Combust. Flame **119**, 203 (1999)
7 J.L. Beduneau, B. Kim, L. Zimmer, Y. Ikeda, Combust. Flame **132**, 653 (2003)
8 T.W. Lee, V. Jain, S. Kozola, Combust. Flame **125**, 1320 (2001)
9 H. El-Rabii, G. Gaborel, J.P. Lapios, D. Thévenin, J.C. Rolon, J.P. Martin, Opt. Commun. **256**, 495 (2005)
10 H. El-Rabii, K. Zähringer, J.C. Rolon, F. Lacas, Combust. Sci. Technol. **176**, 1391 (2004)
11 A. Stakhiv, R. Gilber, H. Kopecek, A.M. Zheltikov, E. Wintner, Laser Phys. **146**, 738 (2004)
12 S.O. Konorov, A.B. Fedotov, O.A. Kolevatova, V.I. Beloglazov, N.B. Skibina, A.V. Shcherbakov, E. Wintner, A.M. Zheltikov, J. Phys. D **36**, 1375 (2003)
13 A.F. Yalin, M. DeFoort, B. Willson, Opt. Lett. **30**, 206 (2005)
14 A. Lemaire, Ph.D. thesis (École Centrale, Paris, 2003)
15 R. Lang, J. Acoust. Soc. Am. **34**, 6 (1962)
16 N.G.R. Broderick, H.L. Offerhaus, D.J. Richardson, R.A. Sammut, J. Caplen, L. Dong, Opt. Fiber Technol. **5**, 185 (1999)
17 R.F. Cregan, B.J. Mangan, J.C. Knight, T.A. Birks, P.S.J. Russell, P.J. Roberts, D.C. Allan, Science **285**, 1537 (1999)
18 T.X. Phuoc, Opt. Lasers Eng. **44**, 351 (2006)
19 D.G. Ouzounov, F.R. Ahmad, D. Müller, N. Venkatamaran, M.T. Gallagher, M.G. Thomas, J. Silcox, K.W. Koch, A.L. Gaeta, Science **301**, 1702 (2003)